S11

Proceedings of the 5th International Conference on Inverse Problems in Engineering: Theory and Practice, Cambridge, UK, 11-15th July 2005

A SEQUENTIAL ULTRASOUND AND ELECTRICAL CAPACITANCE PROCESS TOMOGRAPHY SYSTEM

G. STEINER, D. WATZENIG, B. KORTSCHAK and B. BRANDSTÄTTER
Christian Doppler Laboratory for Automotive Measurement Research located at the
Institute of Electrical Measurement and Measurement Signal Processing,
Graz University of Technology, Kopernikusgasse 24, 8010 Graz, Austria
e-mail: {steiner, watzenig, kortschak}@emt.tugraz.at, brand@ieee.org

Abstract - A novel concept for the fusion of Ultrasound Reflection Tomography (URT) and Electrical Capacitance Tomography (ECT) for industrial process applications is presented. The method is intended to combine the strengths of both principles while reducing their respective disadvantages. ECT is sensitive to bulk rather than to phase boundaries and suffers from blurred images. URT is able to detect phase boundaries with good resolution but is not able to reconstruct absolute material parameters. In our approach URT and nonlinear Gauss-Newton based ECT are sequentially coupled by using the URT results as a natural regularization for the ECT reconstruction algorithm. Two different methods are investigated that can also be simultaneously used. Adaptive mesh grouping uses data from the ultrasonic measurements to merge regions without phase boundaries before performing the ECT inversion, thus reducing the number of unknowns. For the second method a weighted regularization matrix is composed based on the URT data, leading to a physically meaningful regularization. The methods are tested with simulated gas-liquid two-phase flow profiles. The achieved results show a significant improvement compared to stand-alone ECT.

1. INTRODUCTION

Process tomography techniques for monitoring industrial processes have been the subject of extensive research in recent years. Several methods based on different physical effects have been investigated, e.g. electrical capacitance, electrical resistance, ultrasound and optical tomography [17]. All of the aforementioned methods have shown to be potentially useful. However, the achievable resolution and accuracy are limited in practice. In general, the inverse problems are ill-posed. Electrical Capacitance Tomography (ECT) with a nonlinear Gauss-Newton based reconstruction algorithm, for instance, heavily relies on regularization. Authors often use the identity matrix as regularization matrix, penalizing high values for the permittivities, or use a discrete differential operator to incorporate a smoothness assumption on the solution [5]. In both cases the regularization implies some a priori knowledge on the material distribution. This is not correct in a physical sense, since in many cases we have to deal with distributions of piecewise constant permittivities. Such a situation arises in bubbly gas-liquid two-phase flows, where sharp transitions between the two phases exist. The regularization may lead to acceptable reconstruction results but will inherently reduce the achievable resolution and contrast of the reconstructed image.

In order to partly overcome the disadvantages of ECT and to introduce a physically meaningful regularization, we propose to combine ECT with a different tomographic modality with complementary properties. The data obtained from both methods should be fused to yield better overall reconstruction results. Similar approaches were pursued for other tomographic imaging principles. Computed Tomography (CT) X-ray data for the inspection of sandwich structures was fused with laser range and ultrasound thickness measurements by imposing geometrical constraints on the linear equation system for reconstruction [1]. The constraints reduced the degree of ill-posedness of the computed tomography problem and led to an improvement of the reconstructed image. A second approach used Diffuse Optical Tomography (DOT) structurally guided by reconstructive ultrasound tomography [20]. The results from ultrasound tomography were used to locally refine the finite element mesh used for DOT in areas where phase boundaries were detected. As a result, the spatial resolution of the imaging system was considerably improved. This approach was not adopted for the present application in order to maintain the reconstruction speed of ECT. A design study of an integrated multi-modal process tomography system was presented in [6]. Both hardware and software aspects were addressed from a systems engineering point of view.

ECT is sensitive to bulk rather than to phase boundaries. As an advantage, it is possible to reconstruct material properties and to calculate integral parameters, like material fractions, of the process to be monitored. However, sudden phase transitions cannot be detected with most of the existing reconstruction algorithms due to blurring. A tomographic method with almost opposite properties is Ultrasound Reflection Tomography (URT). It is based on the measurement of ultrasonic waves reflected at phase boundaries. Therefore it is sensitive to transitions between the gas phase and the liquid phase. URT has already widely been studied for monitoring industrial processes. Special effort was put on two-phase flows, like bubbly gas-liquid flows, in pipelines [9, 12, 18]. A disadvantage of

URT is that it cannot be guaranteed that the reconstructed phase boundaries are closed contours. This may not be of major concern if one is interested in qualitative images, but seriously complicates the calculation of integral flow parameters. Nevertheless, the available boundary information perfectly supplements the information gathered from capacity measurements and can be used as a "natural" regularization for ECT. Another complementary feature is the distribution of the sensitivity of each method in the region of interest. ECT has the highest sensitivity of electrode potentials with respect to permittivity changes at the margin of the region of interest, while the sensitivity is poor at the center. With URT, objects near the center of the region of interest can be reconstructed with higher contrast than objects close to its border.

A fusion of ECT and URT has not yet been carried out to the knowledge of the authors. Three different principles of combining URT and ECT may be thought of:

- Sequential coupling, by using one method for regularization of the second reconstruction.
- Parallel processing, e.g. through the use of a common cost functional for reconstruction.
- Post-processing, where the reconstruction results of both methods are combined using image processing techniques.

In this paper we will focus on sequential coupling of URT and ECT where the results from URT are used for the regularization of the ECT reconstruction. The second possibility for sequential processing would be to use the ECT results to enhance the URT reconstruction process, e.g. by generating a nonlinear weighting function for filtered backprojection of the reflection measurements. However, this method is not pursued in this work since the reconstruction would still not guarantee closed contours of the phase boundaries.

The paper is organized as follows: In the next two sections we introduce our implementations of ECT and URT. Advantages and disadvantages of the different tomography principles are highlighted in more detail. After that, the fusion of URT and ECT by sequential coupling is addressed. Two methods for the regularization of ECT with URT data are elaborated. Finally, the sequential methods are applied to two simulated test distributions of marsh gas bubbles immersed in oil. The results are compared with stand-alone ECT and URT results.

2. ELECTRICAL CAPACITANCE TOMOGRAPHY (ECT)

ECT is a technique for reconstructing information about the spatial distribution of the cross-sectional area of closed objects by boundary measurements [17]. Depending on the applied reconstruction algorithm, the measurands at the boundary are electrical capacitances or potentials. The region of interest may be, for instance, a pipeline, a chamber or a vessel. Figure 1 illustrates the basic block diagram of an ECT system consisting of a pipe and a ring of 16 electrodes. The electrodes are attached to the surface of the pipe and a predefined voltage pattern is applied. In each measurement cycle two electrodes are active while, in our case, the electrical potentials of the other electrodes are measured. Each electrode can be used as transmitting or receiving electrode. Based on the measured potentials an approximation of the material distribution is computed. The physical relationship between the measured voltages and the permittivity distribution inside the object is governed by a partial differential equation with adequate boundary conditions. The reconstruction algorithms of most ECT systems currently in use are based on the assumption of a linear mapping between permittivity values and measured capacitances. Well known methods are Simultaneous Iterative Reconstruction Technique, Offline Iteration Online Reconstruction and Landweber's iteration method [3, 10, 19]. Even though all of the mentioned reconstruction algorithms are fast, they suffer from blurred images. Another drawback is that linear reconstruction techniques only have a qualitative expressiveness and thus such methods are not suitable when absolute permittivity values are of interest. For all three methods, the blurring of the images occurs mainly because of two reasons: the sensitivity of the measured capacitance with respect to small local variations of the electric permittivity is poor, and the reconstruction algorithms are based on a linear mapping between permittivity and capacitance although this relationship is highly non-linear due to field-strength inhomogeneities and not negligible dimensions of the permittivity perturbation. In order to improve both image quality and reconstructed permittivity accuracy nonlinear methods can be applied. In this paper a Gauss-Newton based reconstruction scheme is utilized [2]. Due to the selection of a predefined electrode switching pattern the proposed method requires less measurements compared to backprojection based systems measuring all inter-electrode capacitances. The selection of the switching pattern is based on a sensitivity analysis with regard to obtaining a uniform sensitivity throughout the pipe.

Applying a Gauss-Newton based reconstruction implies the solution of the forward problem. The forward problem or, underlying field problem, consists of determining the distribution of the electric scalar potential V (and subsequently the electric field strength and the capacitance) for a given permittivity distribution within the pipe. The governing equations are Gauss' and Faraday's law for the static case leading to the following equation in the interior of the pipe:

$$\nabla \cdot (\varepsilon_r \nabla V) = 0, \tag{1}$$

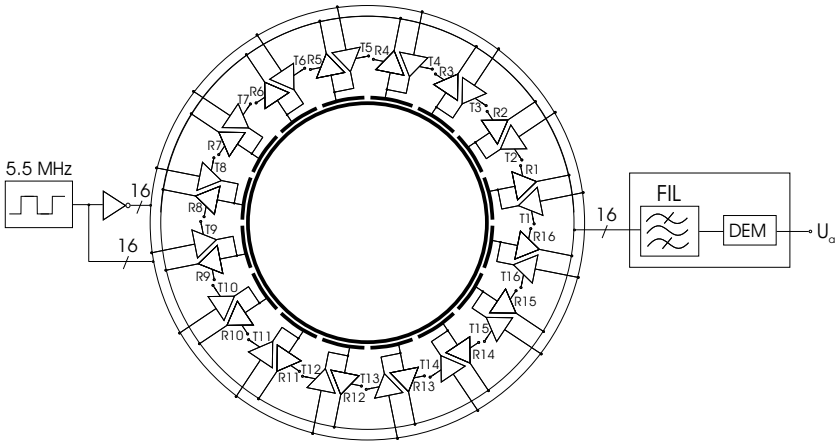

Figure 1: Block diagram of an ECT system. Each of the 16 electrodes can be used as transmitting and receiving electrode. Additionally, the select line for each amplifier is plotted (signals R1-R16, T1-T16). The system is fed by an external oscillator. In order to obtain a 180° phase-shifted signal, the oscillator signal can be inverted. The 16 output voltages corresponding to the 16 electrodes are bandpass filtered and demodulated.

where ε_r is the dimensionless spatially dependent electric permittivity. The partial differential equation (1) is solved by means of a finite element approach. For this purpose the cross-section of the pipe is discretized into 280 linear triangular finite elements. The number of elements within the region of interest is equal to the number of degrees of freedom. The electrodes and the outer space have to be discretized as well, but these elements do not contribute to the complexity of the equation system to be solved.

To determine the permittivity distribution based on the measured potential values at the measurement electrodes, the following inverse problem has to be solved:

$$\varepsilon_r^* = \arg\min_{\varepsilon_r} \left\{ \|V_c - V_m\|_2^2 + \alpha \|L\varepsilon_r\|_2^2 \right\}, \tag{2}$$

where V_m is a vector of measured potentials and α is the regularization parameter. V_c is the vector of iteratively computed potentials. Since the inverse problem is severely ill-posed, the regularization term $\alpha \|L\varepsilon_r\|_2^2$ which is controlled by the regularization parameter has to be introduced. In fact, large values of α lead to a homogeneous permittivity distribution, i.e. the remaining residual $\|V_c - V_m\|_2^2$ will be too large. On the other hand, for small values of α the solution will be dominated by the contributions from data inaccuracies. For obtaining a reasonable solution for a regularized reconstruction problem it is necessary to find a good choice for α. The regularization parameter should yield a fair balance between the two terms in (2). By virtue of the demand on a real time operating algorithm, the regularization term is controlled iteratively according to (3).

$$\alpha_i = \frac{\|V_{c,i} - V_m\|_2^2}{\kappa \|L\, \varepsilon_{r,i}\|_2^2} \tag{3}$$

The regularization parameter α_i is controlled in that way that for a decreasing solution norm $\|V_{c,i} - V_m\|_2^2$ the regularization term $\|L\, \varepsilon_{r,i}\|_2^2$, is forced to get smaller too in each iteration step i of the Gauss-Newton based reconstruction algorithm. The parameter κ is a weighting factor. This adaptive strategy to control the regularization term has been introduced in [15]. Due to the fact that in this work only two-phase fields with permittivity values close to each other (oil and marsh gas) are treated, the rule to control α can be simplified. This means that the starting value of α and the weighting factor κ are chosen a priori to the reconstruction task ($\alpha_0 = 10^{-4}$, $\kappa = 5 \times 10^3$), since these two factors are almost independent of the distribution to be reconstructed. However, the order of magnitude has to be chosen properly.

3. ULTRASOUND REFLECTION TOMOGRAPHY

URT for industrial processes is an imaging technique based on time-of-flight measurements of reflected ultrasonic waves arriving at the boundary of the region of interest. It aims at reconstructing the acoustic reflectivity function of a cross-section of a pipe. It was successfully applied to the identification of bubbly gas-liquid flows [9, 12, 18]. Typically there is a great difference between the acoustic impedance of gases and liquids, resulting in a nearly perfect reflection of sound waves at phase boundaries. For instance, the reflection coefficient at a mineral oil-marsh

gas interface is 99.95%. Gas bubbles can therefore be treated as perfect reflectors as long as their geometrical dimensions are several times larger than the wavelength of the incident ultrasonic wave.

The layout of a URT system for pipelines is similar to that of the ECT sensor depicted in Figure 1. Instead of electrodes, ultrasonic transducers are evenly spaced around the circumference of the pipe. The transducers must be in contact with the medium inside the pipe in order to effectively insonify the region of interest. This can be achieved by slots in the pipe accomodating the ultrasonic transducers. All transducers can be used as both transmitters and receivers. One transducer at a time is excited with a broadband pulse and emits an acoustic wave. This triggers the data acquisition where all transducers simultaneously act as receivers. Typical waveforms simulated for 2 MHz transducers are shown in Figure 2(b). The time-of-flight information of reflected waves is extracted from the recorded waveforms and used for the reconstruction process. The next transducer is used as a transmitter after the sound field has died down. To obtain sufficient information for the reconstruction process it is essential that the transducers have a wide beam angle in the lateral direction. On the contrary the beam should be very narrow in the azimuthal direction to insonify only a thin slice of the pipe. Such characteristics can be achieved by a suitable design of the ultrasonic transducers [13].

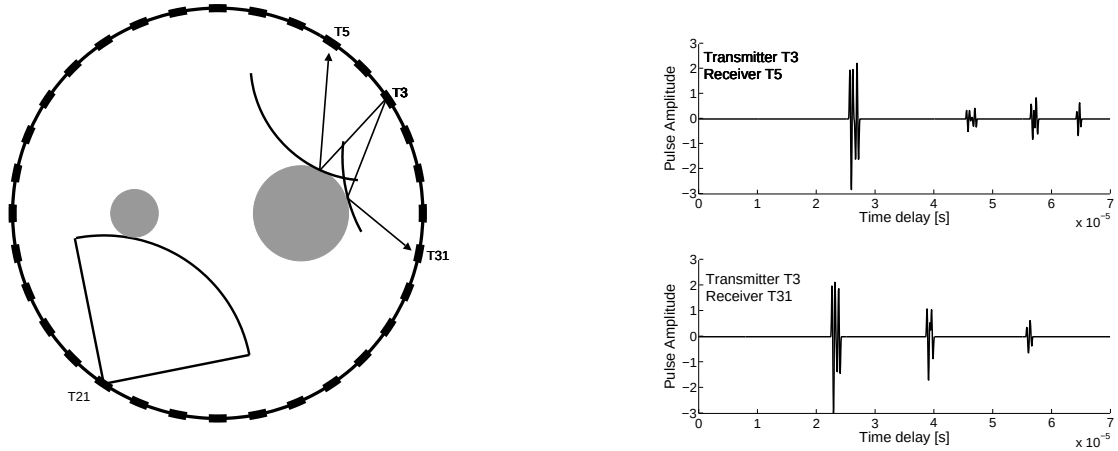

(a) Principle of ultrasound reflection tomography. Received pulses are backprojected on ellipsoidal arcs.

(b) Typical signals simultaneously detected by different receivers while one transducer is active.

Figure 2: Layout, principle and typical sensor signals of an ultrasound reflection tomography system.

The reconstruction is performed by means of a simple backprojection of the recorded arrival times. This is indicated in Figure 2(a). The illustration shows a URT sensor with 32 transducer elements enclosing a region of interest containing two gas bubbles. A wide beam ultrasonic pulse emitted by the transducer T21 is partly reflected back to T21 at the first bubble. From the measured time-of-flight a circular arc can be backprojected. A second situation is depicted in the right part of the pipe. A pulse emitted by T3 is e.g. reflected towards T5 and T31. The signal received by a transducer depends on the reflectivity function $f(x, y)$ in the interior of the pipe,

$$u_{T_t,T_r}(t) = p(t) * \int_{a_{T_t,T_r}(t)} b_{T_t}(x, y)\, b_{T_r}(x, y)\, f(x, y) ds \tag{4}$$

where the subscripts T_t and T_r denote the transmitting and receiving transducer and $p(t)$ is the impulse response of transmitter, receiver and electronic circuitry. The symbol '$*$' denotes the convolution operation. The functions b_{T_t} and b_{T_r} account for the angular dependence of the transmission and reception sensitivities of the transducers. The elliptic integration path $a_{T_t,T_r}(t)$ spreads with increasing time. The backprojections take the form of ellipsoidal arcs with the foci at the transmitting and receiving transducers, respectively. The reconstruction is obtained by summing up all backprojections and applying a threshold filter. In general, the reconstructed images suffer from blurring. This effect can be reduced by reconstruction with a filtered backprojection algorithm [11]. However, this method is not employed in the present work to keep the computational requirements of URT low. The reconstruction is performed on an image matrix with 100×100 pixels in our case.

The large number of parallel measurement channels results in high hardware requirements. Empirical studies have shown that at least 30 transducers are necessary to obtain reasonable images [12,14]. However, for the present application where URT data is used to improve the ECT solution, the quality of the URT image is not the major concern. It was found that a number of 16 ultrasonic transducers is able to produce sufficient information to considerably improve the subsequent permittivity reconstruction. Typical URT images obtained with 16 transducers

are shown in Figures 3(a) and 6(a).

4. FUSION OF ULTRASOUND AND CAPACITANCE TOMOGRAPHY

According to the classification noted in the introducing section, there are three different kinds of combining URT and ECT. The current work concentrates on the sequential fusion of URT and ECT when two-phase flow fields have to be analyzed. The idea is to fuse both tomographic systems in that way to bring out their respective advantages. URT has the benefit of detecting edges accurately, while it is not possible to reconstruct permittivity values of the involved materials. ECT with nonlinear iterative reconstruction, on the other hand, enables the quantification in terms of absolute permittivity values. However, due to needful regularization, no sharp edges can be resolved. Thus, a combination of both is reasonable. The sensor fusion is done by using the result of URT as a priori information for ECT. In order to combine URT and ECT sequentially, two different approaches, adaptive mesh grouping and weighting of the regularization matrix, are investigated.

4.1. Adaptive Mesh Grouping

A major problem when applying a Gauss-Newton algorithm to solve the inverse ECT problem is the superproportional dependence between the increasing number of elements in the region of interest and the increasing computational effort. On the one hand, an increase of the number of unknowns improves the spatial resolution of the reconstructed cross-sectional images, but, on the other hand, the convergence characteristics are downgraded considerably. In order to overcome these drawbacks in case of a two-phase field, various mesh grouping methods have been proposed [4, 7]. When meshes are appropriately grouped, the number of unknowns can be reduced without sacrificing the spatial resolution. In the mesh grouping approaches the knowledge that there are only two representative permittivity values is exploited. The intermediate permittivity values obtained from the Gauss-Newton or Newton-Raphson based reconstruction are examined and can be classified into three groups such as target group, background group and unadjusted group. After classification, the Gauss-Newton algorithm is modified in order to decrease the number of unknowns iteratively. Ideally, after terminating the reconstruction task, there should be no element in the unadjusted group, since all elements are reassigned to either background group or target group. The main disadvantage of this method is to define an upper and lower threshold for the permittivity values in order to reassign the elements within the unadjusted group. So far, the threshold levels have to be found out by trial and error.

Applying URT prior to the ECT enables the opportunity to reduce the parameter space, i.e. the number of unknowns, in a physically meaningful way. Homogeneous parts of the region of interest with constant permittivity values can be identified with URT. For every transmitting transducer of the URT sensor the first echo received by the respective transducer is analyzed. The material distribution must be homogeneous in the beam region that can be backprojected from the first echo. This situation is depicted in the lower left part of Figure 2(a). Thus, the finite elements located in this region can be merged to one large element with one assigned permittivity value. As a result the number of unknowns can be reduced considerably. However, the success of this method depends on the size and number of bubbles within the pipe.

4.2. Weighted Regularization Matrix

Another possibility to improve the image quality is to manipulate the regularization matrix, which is in many cases a discrete Laplacian operator incorporating a smoothness assumption. The regularization is mandatory to manage the ill-posedness of the inverse problem even when this a priori information is wrong in a physical sense.

The regularization matrix L in the present case is a discrete differential operator where

$$L(i,j) = \begin{cases} -1 & \text{when finite element } j \text{ is a neighbor of finite element } i \\ 0 & \text{otherwise} \end{cases} \tag{5}$$

The diagonal elements of the regularization matrix L are given by

$$L(i,i) = -\sum_{j,i\neq j} L(i,j) \tag{6}$$

This choice of the matrix incorporates a smoothness assumption about the interior region into the mathematical model. This kind of regularization is also known as Tikhonov's regularization.

Performing URT in the case of a two-phase field can also be used to detect edges between regions of different permittivity values. If URT is performed on the finite element mesh used for ECT instead of on a regular pixel

grid, a unique allocation of occurring edges and corresponding finite elements is possible. With this knowledge the regularization matrix used in ECT can be manipulated by weighting the corresponding elements. In other words, the smoothness assumption is suspended in areas where the URT has detected edges. The conventional regularization matrix (5) is replaced with

$$L(i,j) = \begin{cases} -w(i) & \text{when finite element } j \text{ is a neighbor of finite element } i \\ 0 & \text{otherwise} \end{cases} \tag{7}$$

$$w(i) \quad = \quad 1 - \frac{u(i)}{\max\limits_{j} \{u(j)\}} \tag{8}$$

where $w(i)$ is a weighting factor which depends on the reconstruction result of URT. In order to find elements which correspond to edges, URT is performed on the finite element mesh used for ECT. The reconstructed edge intensity of an element i in the region of interest is denoted by $u(i)$. In particular, for the element with the largest value the regularization is set to zero, while the other elements are weighted according to (8).

In this paper both of the above mentioned methods are utilized. Furthermore, the combination of adaptive mesh grouping and weighted regularization matrix is exploited. The validation of the different approaches is illustrated and discussed in the following section by means of two test distributions.

5. SIMULATION RESULTS

In order to testify the proposed sequential tomographic systems, two different artificial test distributions are chosen. The first distribution, *distribution 1*, shows a gas bubble ($\varepsilon_r = 1$) in oil ($\varepsilon_r = 2$), while the second one, *distribution 2*, depicts two gas bubbles in oil with the same dielectric properties. The inner diameter of the pipe is 70 mm. Bubble diameters of 16 and 8 mm were assumed.

The measurement data needed as input for the reconstruction algorithms were synthetically generated. The ultrasonic forward problem was simulated with a ray-tracing technique similar to that described in [16]. In addition, several characteristics of real-life systems were modelled: impulse responses of the transducers and amplifiers, nonuniform acoustic beam profiles and transducer sensitivities, beam attenuation, sampling and time-of-flight extraction by thresholding. The simulations were carried out with typical parameters for a 2 MHz PZT transducer and a -10dB beam angle of 90°.

The simulated measurement data for ECT is obtained by solving a coupled Boundary Element Method (BEM) and Finite Element Method (FEM) problem [8]. The electrodes, the PVC tube and the outer space are discretized into linear triangular elements while in the interior of the pipe the BEM is applied. Using the BEM in the region of interest increases the accuracy of the simulation since the discretization error due to finite elements is avoided. In contrast to the measurement simulation the ECT reconstruction is performed using a finite element discretization of the problem region. Both ultrasonic and capacitive measurements are simulated without additional measurement noise in this first approach.

5.1. Distribution 1

This simple test distribution consists of a single gas bubble located in the upper right part of the pipe. The reconstruction results with URT and ECT independently applied are illustrated in Figure 3. The ECT image is obtained by linear interpolation of the finite element values. The URT image was obtained from the reduced configuration with 16 transducers that is also used for the fusion with ECT. The image is slightly blurred and already exhibits the disadvantage of URT that closed contours cannot be guaranteed. The stand-alone ECT reconstruction is shown as a contour plot of the reconstructed permittivity distribution in Figure 3(b). The numbers indicate relative permittivity values. The reconstruction suffers from significant blurring due to the imposed smoothness assumption. The performance of the sequential adaptive mesh grouping and weighted regularization matrix methods in comparison with conventional ECT are illustrated by a horizontal intersection line through the image plane through the center of the bubble. The fusion based on adaptive mesh grouping only, depicted in Figure 4(a), yields a considerable improvement. The size and permittivity of the original bubble are matched much better and the blurring is significantly reduced. In addition, the reconstructed permittivity distribution in the oil fraction is flatter than with conventional ECT due to the mesh grouping. Figure 4(b) shows the results when the weighted regularization matrix only is used for fusion. It can be seen that the original distribution is better matched than with normal ECT in all parts of the cross-section, but the improvement is not as significant as with adaptive mesh grouping. Finally, both adaptive mesh grouping and weighted regularization matrix were simultaneously applied. The results are contained in Figure 5. As is obvious from Figure 5(a) the combination of adaptive mesh grouping and weighted regularization matrix offers hardly any improvement compared with simple adaptive mesh grouping fusion for this

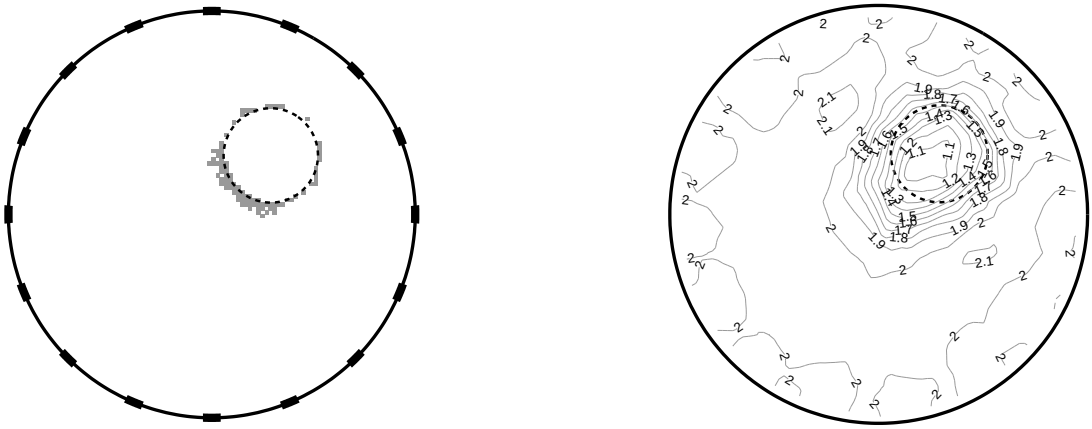

(a) Reconstruction result with URT using 16 transducers

(b) Reconstruction result with ECT using 16 electrodes

Figure 3: Reconstructed images with URT and ECT. In addition, the true test distribution is plotted (black dashed circle).

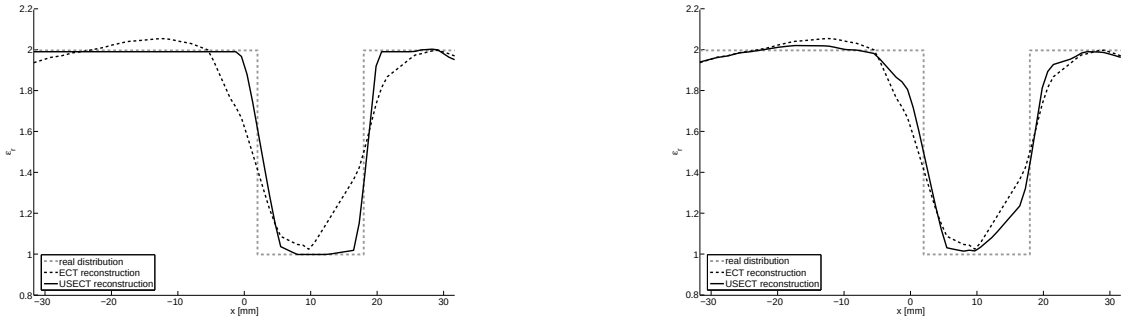

(a) Reconstruction result with adaptive mesh grouping

(b) Reconstruction result with modified L-matrix

Figure 4: Intersection line through the center of the bubble. The figures compare the results achieved with ECT and the results achieved with (a) adaptive mesh grouping and (b) weighted regularization matrix. The gray dashed line depicts the true test distribution.

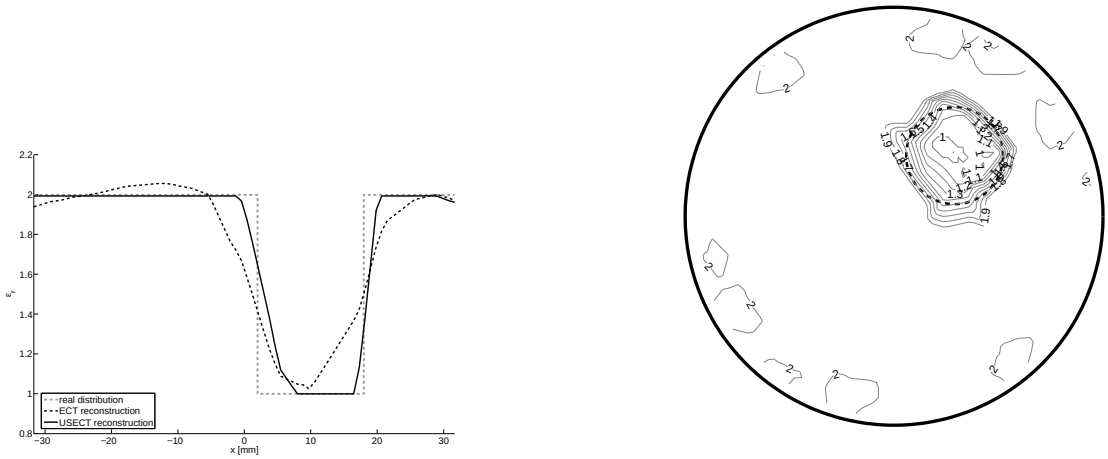

(a) Reconstruction result with both methods combined

(b) Reconstruction result with both methods combined

Figure 5: Intersection line through the center of the bubble on the left and contour plot on the right when adaptive mesh grouping and weighted regularization matrix are used in combination.

particular problem. Compared with the conventional ECT image, the fused reconstruction of Figure 5(b) is cleary superior. The blurring is substantially reduced and the image offers a good reconstruction of the real situation.

5.2. Distribution 2

The second test distribution consists of a large and a small bubble immersed in oil. Figure 6 shows the reconstruction results from stand-alone URT and ECT. URT is able to recover a wide part of the interfaces between oil and gas. However, some gaps, especially for the small bubble, and artefacts are present in the image. ECT alone is hardly capable of resolving the two bubbles. Only a small cavity at the position of the small bubble can be identified from Figure 6(b). The application of sequential fusion with either adaptive mesh grouping or weighted regularization matrix results in a distinctly improved separation of the bubbles, as can be seen from Figure 7. In addition the permittivity of the larger bubble is correctly reconstructed. adaptive mesh grouping also leads to a better match of the permittivities in the region outside the bubbles. The best results can be achieved with the application of both adaptive mesh grouping and weighted regularization matrix, which is illustrated in Figure 8. Compared with stand-alone ECT the quality of the reconstruction can be significantly improved. The two bubbles can now be clearly separated and the blurring is reduced. The spatial resolution of the small bubble is worse than that of the large bubble. This is caused by the size of the finite elements with edge lengths equal to the diameter of the small bubble.

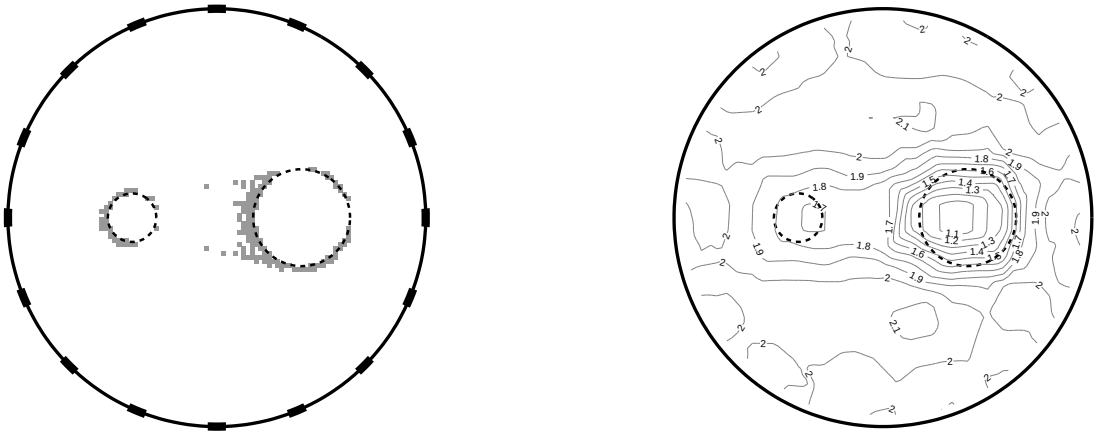

(a) Reconstruction result with URT using 16 transducers

(b) Reconstruction result with ECT using 16 electrodes

Figure 6: Reconstructed images with URT and ECT. In addition, the true test distribution is plotted (black dashed circle).

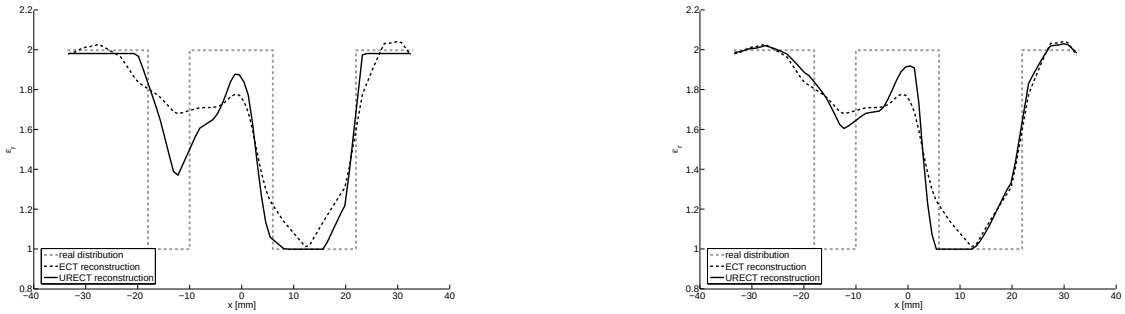

(a) Reconstruction result with adaptive mesh grouping

(b) Reconstruction result with modified L-matrix

Figure 7: Intersection line through the center of the bubbles. The figures compare the results achieved with ECT and the results achieved with (a) adaptive mesh grouping and (b) weighted regularization matrix. The gray dashed line depicts the true test distribution.

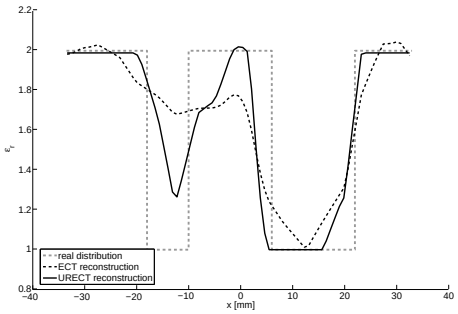

(a) Reconstruction result with both methods combined

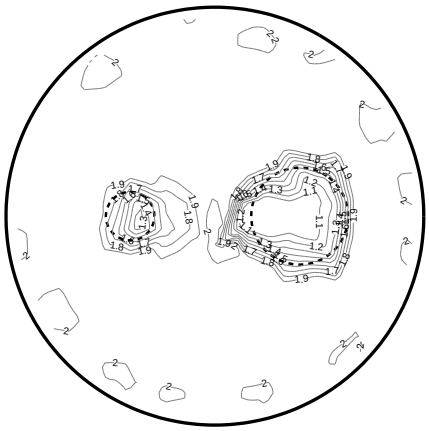

(b) Reconstruction result with both methods combined

Figure 8: Intersection line through the center of the bubbles on the left and contour plot on the right when adaptive mesh grouping and weighted regularization matrix are used in combination.

6. CONCLUSION

In this paper a novel method for image reconstruction of two-phase flow fields in industrial process tomography by means of sequential coupling of an ultrasonic tomography system with an ECT system is proposed. Applying sensor fusion enables to elaborate and to combine the advantages of both tomography systems, yielding remarkably better results than utilizing only one tomographic system. Since ECT is sensitive to bulk rather than to phase boundaries, it is reasonable to introduce a tomographic modality with complementary properties. Combining ECT with URT enables both the reconstruction of material properties and the inclusion of physically meaningful regularization to the ECT based reconstruction task. In fact, URT is performed prior to get a starting guess for the subsequently utilized ECT. In order to incorporate the information provided by URT, two different approaches, adaptive mesh grouping and weighting of the regularization matrix, are investigated and compared. Both methods cause barely no additional computational effort which is particularly important in industrial process tomography, where real time reconstruction is required. As a result, it depends on the distribution to be reconstructed, which one of the two methods performs better in terms of spatial resolution and achievable accuracy. However, the best overall results can be obtained when combining both. Future work will concentrate on the verification of the proposed sequential coupling of URT and ECT with real measurement data.

REFERENCES

1. J.E. Boyd and J.J. Little, Complementary data fusion for limited-angle tomography. *J. Nondestruct. Eval.* (1995), **14**, 61-76.

2. B. Brandstätter, G. Holler and D. Watzenig, Reconstruction of inhomogeneities in fluids by means of capacitance tomography. *COMPEL* (2003), **22**, 508-519.

3. B. Brandstätter, G. Holler and D. Watzenig, Reconstruction of the spatial distribution of water in oil by means of capacitance tomography - a comparison of techniques, *Fifth International Conference on Electromagnetic Wave Interaction with Water and Moist Substances (ISEMA2003)*, Rotorua, New Zealand, 23-26 March, 2003, pp.79-84.

4. K.H. Cho, S. Kim and Y.J. Lee, Impedance imaging of two-phase flow field with mesh grouping method. *Nucl. Eng. Des.* (2004), **204**, 57-67.

5. P.C. Hansen, *Rank-deficient and discrete ill-posed problems*, Society for Industrial and Applied Mathematics (SIAM), Philadelphia, 1998.

6. B.S. Hoyle, X. Jia, F.J.W. Podd, H.I. Schlaberg, H.S. Tan, M. Wang, R.M. West, R.A. Williams and T.A. York, Design and application of a multi-modal process tomography system. *Meas. Sci. Technol.* (2001), **12**, 1157-1165.

7. K.Y. Kim, B.S. Kim, M.C. Kim, S. Kim, Y.J. Lee, H.J. Jeon, B.Y. Choi and M. Vauhkonen, Electrical impedance imaging of two-phase fields with an adaptive mesh grouping scheme. *IEEE T. Magn.* (2004), **40**, 1124-1127.

8. B. Kortschak and B. Brandstätter, A FEM-BEM approach using level-sets in tomography, *Eleventh International IGTE Symposium on Numerical Field Calculation in Electrical Engineering*, Graz, Austria, 13-15 Sept., 2004, pp.301-307.

9. W. Li and B.S. Hoyle, Ultrasonic process tomography using multiple active sensors for maximum real-time performance. *Chem. Eng. Sci.* (1997), **52**, 2161-2170.

10. S. Liu, L. Fu, W.Q. Yang, H.G. Wang and F. Jiang, Prior-online iteration for image reconstruction with electrical capacitance tomography. *IEE P.-Sci. Meas. Tech.* 2004, **151**, 195-200.

11. M. Moshfegi, Ultrasound reflection-mode tomography using fan-shaped-beam insonification. *IEEE T. Ultrason. Ferr.* (1986), **33**, 299-314.

12. H.I. Schlaberg, M. Yang and B.S. Hoyle, Ultrasound reflection tomography for industrial processes. *Ultrasonics* (1998), **36**, 297-303.

13. H.I. Schlaberg, M. Yang, B.S. Hoyle, M.S. Beck and C. Lenn, Wide-angle transducers for real-time ultrasonic process tomography imaging applications. *Ultrasonics* (1997), **35**, 213-221.

14. H.I. Schlaberg, M. Yang and B.S. Hoyle, Real-time ultrasonic process tomography for two-component flows. *Electron. Lett.* (1996), **32**, 1571-1572.

15. D. Watzenig, B. Brandstätter and G. Holler, Adaptive regularization parameter adjustment for reconstruction problems. *IEEE T. Magn.* (2004), **40**, 1116-1119.

16. F. Wiegand and B.S. Hoyle, Simulations for parallel processing of ultrasound reflection-mode tomography with applications to two-phase flow measurement. *IEEE T. Ultrason. Ferr.* (1989), **36**, 652-660.

17. R.A. Williams and M.S. Beck, *Process tomography, principles, techniques and applications*, Butterworth-Heinemann Ltd., Oxford, 1995.

18. M. Yang, H.I. Schlaberg, B.S. Hoyle, M.S. Beck and C. Lenn, Real-time ultrasound process tomography for two-phase flow imaging using a reduced number of transducers. *IEEE T. Ultrason. Ferr.* (1999), **46**, 492-501.

19. W.Q. Yang, D.M. Spink, T.A. York and H. McCann, An image reconstruction algorithm based on Landweber's iteration method for electrical capacitance tomography. *Meas. Sci. Technol.* (1999), **10**, 1065-1069.

20. H. Zhao, X. Gu and H. Jiang, Imaging small absorbing and scattering objects in turbid media using diffuse optical tomography structurally guided by reconstructive ultrasound tomography. *Opt. Commun.* (2004), **238**, 51-55.